THE UNIVERSITY OF MICHIGAN
COLLEGE OF ENGINEERING
Department of Electrical Engineering
Space Physics Research Laboratory

Scientific Report No. 1

THE THERMOSPHERE PROBE EXPERIMENT

D. R Taeusch
G. R. Carignan
H. B. Niemann
A. F. Nagy

ORA Project 07065

under contract with:

NATIONAL AERONAUTICS AND SPACE ADMINISTRATION
GODDARD SPACE FLIGHT CENTER
CONTRACT NO. NAS 5-9113
GREENBELT, MARYLAND

administered through:

OFFICE OF RESEARCH ADMINISTRATION ANN ARBOR

March 1965

TABLE OF CONTENTS

LIST OF FIGURES

1. DESCRIPTION OF EXPERIMENT

1.1 INTRODUCTION

The thermosphere probe (TP) experiment described herein is the result of a research effort implemented by this laboratory under contract with the NASA Goddard Space Flight Center, Aeronomy and Meteorology Division. The purpose of this effort was to provide an ejectable rocket-borne system capable of making simultaneous direct measurements of gas temperature and density, ion and electron density, and electron temperature in the earth's atmosphere in the altitude region between 100 and 350 km, a region within the thermosphere. The primary mission of the experiment is to fill the present measurement gap in this general altitude region which is above the altitude capability of the grenade, falling sphere and pitot-static techniques, and below the altitude of usual satellite measurements.

The TP incorporates an omegatron partial pressure gage,[1] a cylindrical electrostatic probe,[2] and a sun-earth aspect measuring system. This complement of instruments provides data for the determination of the previously mentioned desired atmospheric parameters. Subsequent development of the aspect determination system permits an extension of the experiment to determine the horizontal component of atmospheric wind in the plane of tumble of the TP.

The ejectable system was chosen for the purpose of removing the TP from the environment of the launch vehicle, similar to the established "Dumbbell" technique,[2] and to permit a tumbling motion to be imparted to the package, independent of the launch vehicle.

The following report describes the theoretical background and techniques utilized in obtaining the gas temperature and density data, the electron temperature and density data, and atmospheric winds. Only those engineering particulars that bear directly on the actual measurement of the desired quantities required for data analysis are described in this report. A comprehensive engineering report of the system is in preparation.

1.2 THE THERMOSPHERE PROBE

The TP is a cylindrical instrument 6 in. in diam, 32 in. long and weighs 40 lb. A photograph of the assembled instrument is shown in Fig. 1. One end of the cylinder contains the omegatron gauge with its circular orifice and breakoff device on the cylindrical axis; the other end of the cylinder contains the earth sensor. The center section contains the sun aspect sensor,

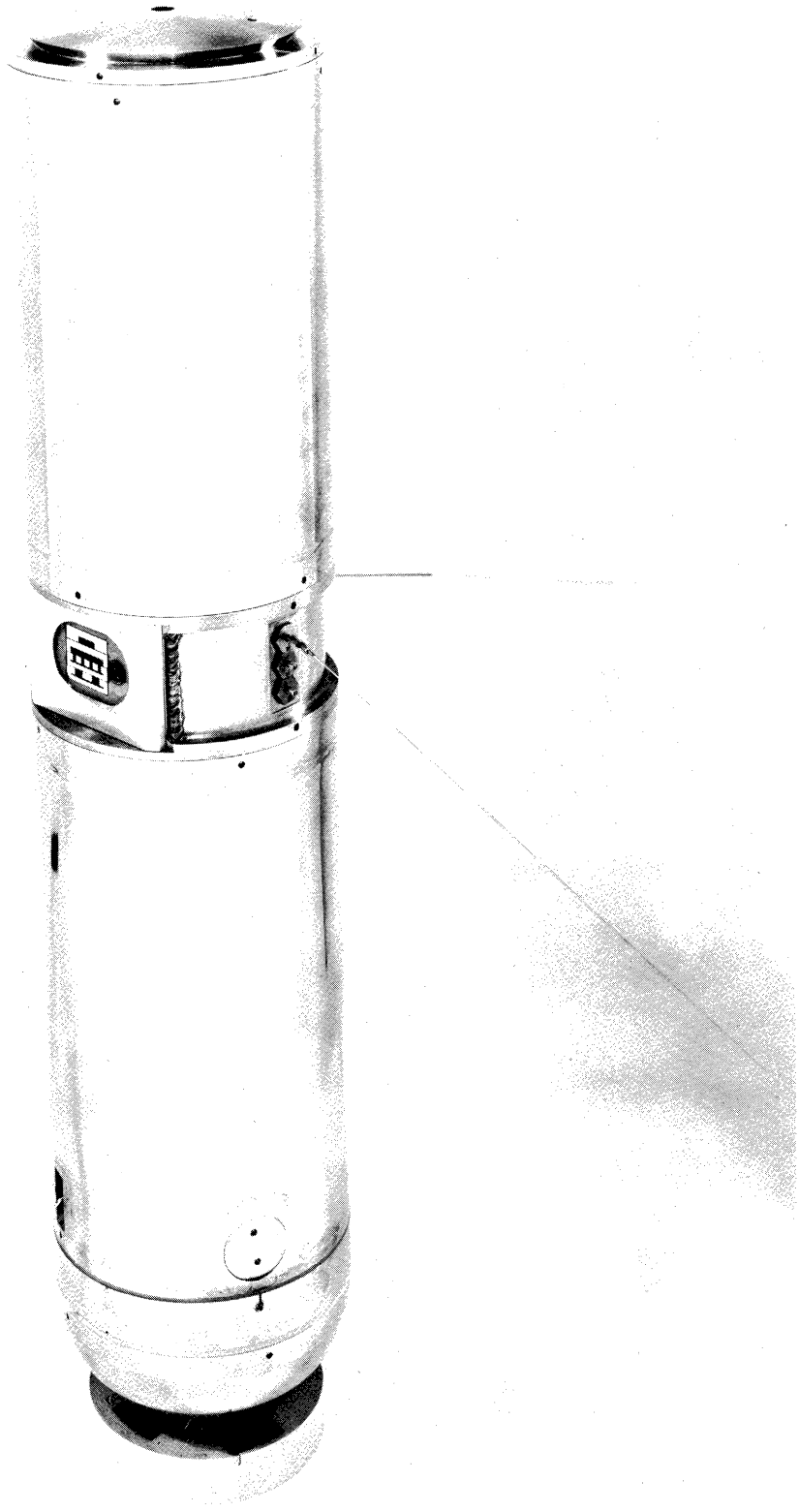

Fig. 1. Assembled TP.

a small cylindrical electrostatic probe and the telemetry antennae. The outer structure of the probe is made of stainless steel and the assembled instrument is vacuum sealed. The probe system is completely self-contained providing its own power supply, measuring sensors, signal conditioning, and transmission equipment.

1.3 EJECTION AND TUMBLE SYSTEM

The ejection nose cone system is shown in Fig. 2. The clamshell-type nose cone halves, which provide the aerodynamic shape of the rocket during powered flight are hinged to the base of the enclosure and are held together against the force of two springs by a magnesium ring which is pyrotechnically fractured to effect opening. The TP rests on a spring-loaded plunger within the enclosure. The plunger is held depressed against the spring force by a latch mechanically linked to a nose cone half so that opening of the nose cone releases the latch, freeing the plunger, which, operating against the compressed spring, ejects the TP from the opened enclosure. A negator motor (constant force spring), with 8 ft of cable is mounted below the plunger. One end of the cable is fastened to the top side of the TP. As the TP leaves the vehicle, it is tumbled in the plane containing the cable hook and the center of gravity. When the TP has tumbled approximately 135°, the cable releases and is reeled back into the vehicle.

The ejection system causes the TP to separate from the nose cone at about 5 fps and the negator or constant force spring imparts the tumble motion with a period of 2.0 sec. The roll period is noncontrolled and is the resultant of the roll period of the rocket at ejection. The opening of the nose cone halves prior to ejection provides an effective despin mechanism assuring a roll rate substantially less than the tumble rate. Thus, with a low roll rate and a moment of inertia ratio of more than 30, the TP can be considered to be tumbling in the plane of the cylindrical axis.

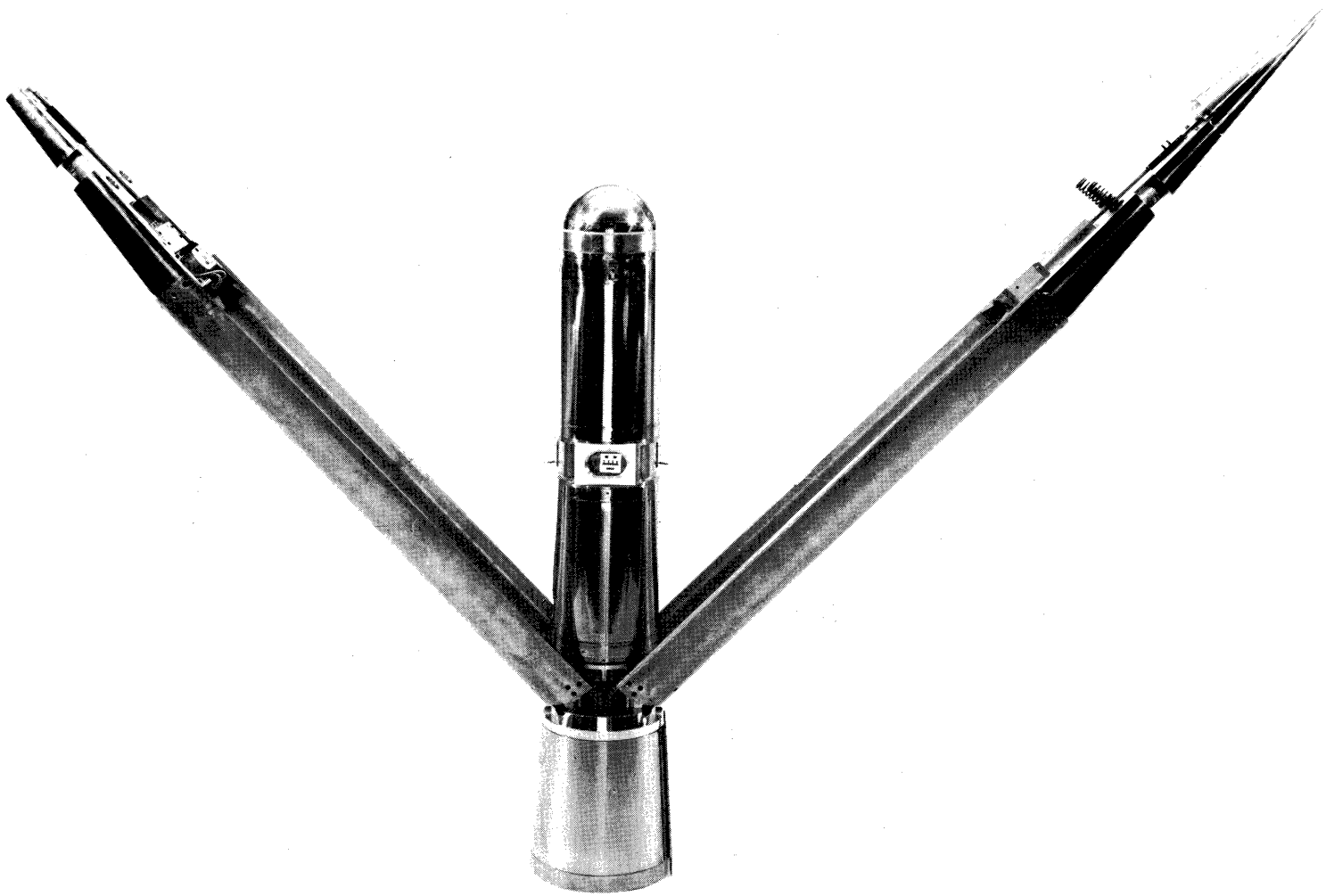

Fig. 2. Ejection nose cone system.

2. ASPECT DETERMINATION

2.1 INTRODUCTION

The analysis of the neutral particle-pressure measurement requires that the orientation of the pressure-gauge orifice, with respect to the velocity vector, be known. For this purpose, the TP experiment utilizes a sun-earth aspect sensor.

The sun aspect sensor views a fan, 360° wide, the plane of which is oriented perpendicular to the long axis of the TP. As the TP tumbles, and rolls, the fan sweeps out a solid angle of 4π steradians, thereby viewing the sun at periodic intervals (every half tumble period). The output of the sun sensor yields the roll position of the TP at the time the sun is viewed.

As was described in a previous section of this report, the ejection system for the TP is designed to decrease the roll rate and tumble the instrument in the plane containing the cylindrical axis. Since there are no external torques on the TP after ejection, it will be assumed that the angular momentum vector, $\bar{L}$, for the system will remain fixed in inertial space.

2.2 EJECTION KINEMATICS

In Fig. 3 the quantities and coordinates of interest are described for the analysis of the equations of motion of the TP during ejection.

The Lagrangian $\mathcal{L}$ for the TP after it has left the plunger is:

$$\mathcal{L} = 1/2m\dot{x}^2 + 1/2I\dot{\theta}^2 - K(x + \epsilon \cos\theta) \qquad (2.2.1)$$

where

I = maximum moment of Inertia

K = constant force spring constant

m = mass of TP

The equations of motion are

$$m\ddot{x} + K = 0 \qquad (2.2.2)$$

and

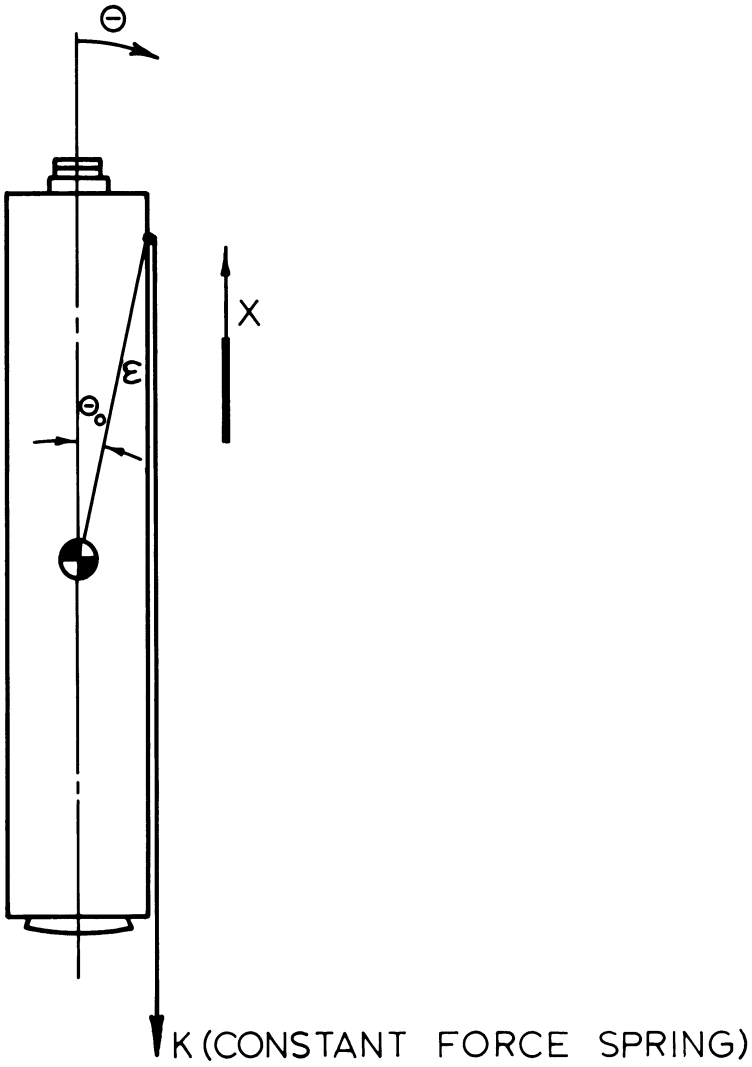

Fig. 3. Ejection kinematics coordinates.

$$I\ddot{\theta} - K\epsilon \sin\theta = 0 \qquad (2.2.3)$$

The solutions to 2.2.1 are:

$$\dot{x} = -\frac{K}{m}t + V_o \qquad (2.2.4)$$

and

$$x = -1/2\,\frac{K}{m}t^2 + V_o t + x_o \qquad (2.2.5)$$

The solutions to 2.2.3 are:

$$\omega_{max} \equiv \dot{\theta}_{max} = \sqrt{2}\,\lambda\,\sqrt{\cos\theta_o - \cos\theta_{max}} \qquad (2.2.6)$$

where θ_{max} = release angle

$$\lambda^2 = \frac{K\epsilon}{I}$$

The release time is:

$$t_{max} = \frac{1}{\sqrt{2}\lambda}\int_{\theta_o}^{\theta_{max}} \frac{d\theta}{\sqrt{\cos\theta_o - \cos\theta}}$$

$$t_{max} = \frac{\beta}{\lambda}F(k,\phi) \qquad (2.2.7)$$

where $\beta^2 = \frac{1}{1-\alpha^2}$; $\alpha = \sin\frac{\theta_o}{2}$; $k = \sin^{-1}\frac{1}{\beta}$

$F(k,\phi)$ = Elliptic Integral of the first Kind.

$$\cos\phi = \frac{\sin\frac{\theta_o}{2}}{\sin\frac{\theta}{2}}$$

The translational velocity of the TP after being tumbled is given by

$$V_{min} = V_o - \frac{\sqrt{2}\,\lambda\, t_{max}}{m}\sqrt{\frac{KI}{2\epsilon}} \qquad (2.2.8)$$

where V_o is the initial velocity obtained from the plunger, which is

$$V_o = \sqrt{\frac{K_p(x^2_{max} - x^2_{min}) - 2Kx_o}{m}} = \sqrt{\frac{2}{m}\,(\text{Energy In})} \qquad (2.2.9)$$

where K_p = plunger spring constant

x_{max} = expanded length of plunger spin

x_{min} = compressed length of plunger spring

$x_o = (x_{max} - x_{min})$

In the present configuration, the TP parameters are:

$m = 1.27$ slugs

$I_{max} = 1.25$ slug ft^2

$I_{min} = .04$ slug ft^2

$K_p = 100$ lb/in

$k = 4$ lb

Energy In $= 61.5$ slug ft^2/sec^2

For the solutions we get

$\epsilon = .97$ ft

$\theta_o = 15°$

$\theta_{max} = 135°$

$\lambda^2 = 3.10$

$\alpha = .1305$

$\beta^2 = 1.017$

$F(82°21', 82°34') = 2.60$

The solutions are:

$V_o \simeq 9.8$ ft/sec

$t_{max} \simeq 1.53$ sec

$V_{min} \simeq 5$ ft/sec

$W_{max} \simeq 3.2$ rad/sec

Tumble Period $= \tau_{max} \simeq 2$ sec

2.3 EQUATIONS OF MOTION OF THE FREE TP

The TP cylinder is assumed to be a symmetrical top moving in a force free space. Referring to Figs. 4 and 5, the 1',2',3' axes of a right Cartesian coordinate system are fixed to the TP, and the 1,2,3 axes are fixed in inertial space. The components of angular velocity along the 1',2',3' axes with respect to the inertial frame of reference in terms of Eulerian angles are:

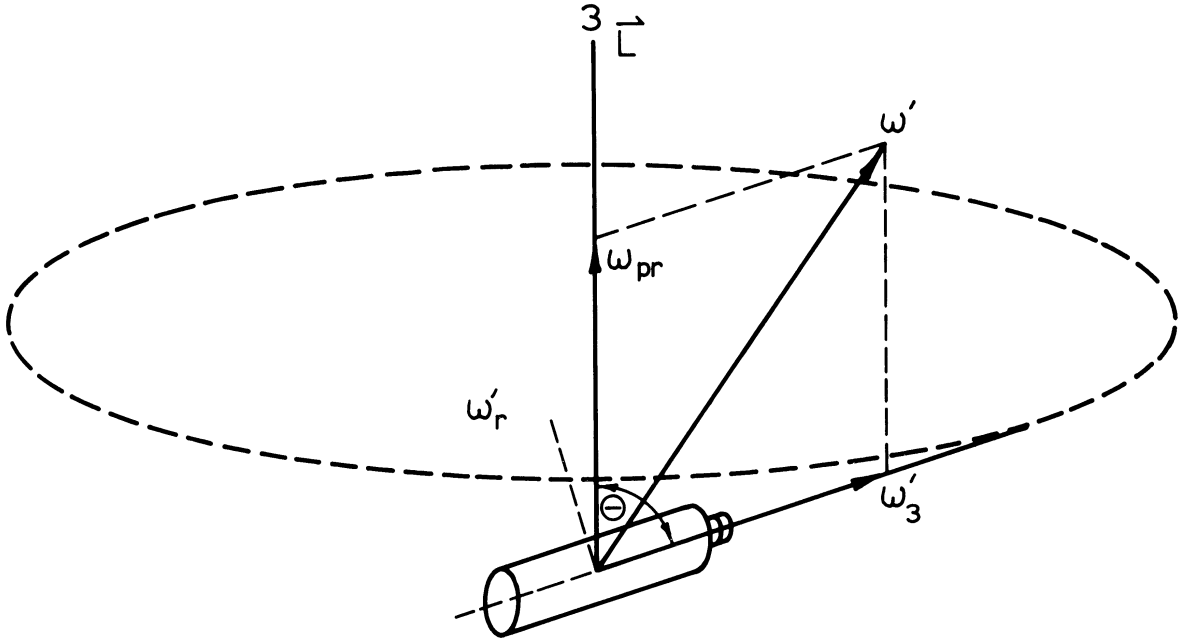

Fig. 4. Coordinates for free TP analysis.

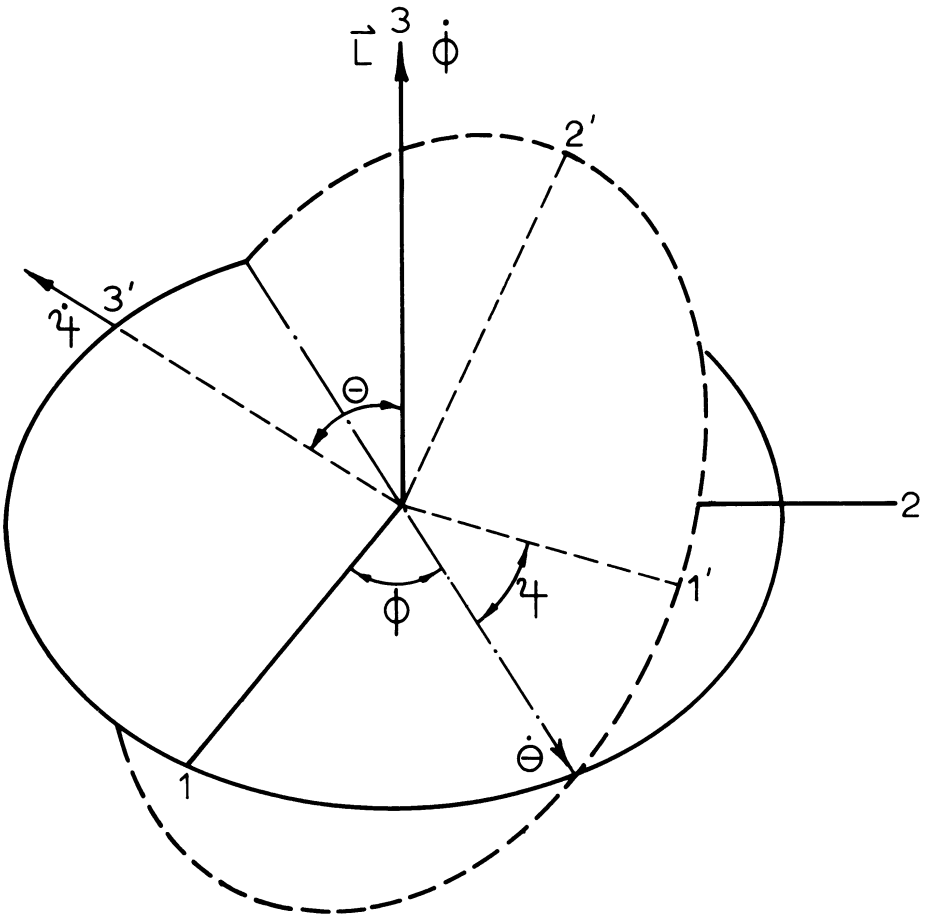

Fig. 5. Coordinates for free TP analysis.

$$\omega_1' = \dot{\phi} \sin\theta \cos\psi + \dot{\theta} \cos\psi$$

$$\omega_2' = \dot{\phi} \sin\theta \cos\psi - \dot{\theta} \sin\psi \qquad (2.3.1)$$

$$\omega_3' = \dot{\phi} \cos\theta + \dot{\psi}$$

The components of the angular momentum for this angular velocities are:

$$L_1' = \omega_1' I_1$$

$$L_2' = \omega_2' I_1 \qquad (2.3.2)$$

$$L_3' = \omega_3' I_3$$

and

$$L^2 = L_1'^2 + L_2'^2 + L_3'^2 \qquad (2.3.3)$$

Assuming the angular momentum vector, $\bar{L}$, is in the direction of the 3 axis of the inertial coordinate system, the components of $\bar{L}$ on the 1',2',3' axes are:

$$L_1' = L \sin\theta \sin\psi$$

$$L_2' = L \sin\theta \cos\psi \qquad (2.3.4)$$

$$L_3' = L \cos\theta$$

Therefore, from (2.3.2) and (2.3.4)

$$\omega_1' = \frac{L}{I_1} \sin\theta \sin\psi$$

$$\omega_2' = \frac{L}{I_1} \sin\theta \cos\psi \qquad (2.3.5)$$

$$\omega_3' = \frac{L}{I_3} \cos\theta$$

Defining ω_r' as the angular velocity along the axis of maximum moment of inertia, we have:

$$\omega_r' = (\omega_1'^2 + \omega_2'^2)^{1/2} = \frac{L}{I_1} \sin\theta \qquad (2.3.6)$$

ω_3' is the angular velocity along the axis of minimum moment of inertia.

The angular velocity is the direction of the 3 axis is the precission angular frequency:

$$\omega_{PR} = \dot{\phi} = \frac{L}{I_1} \tag{2.3.7}$$

From (2.3.1) and (2.3.5)

$$\begin{aligned}
(I_1\dot{\phi}-L)\sin\theta \sin\psi &= -I_1\dot{\theta}\cos\psi \\
(I_1\dot{\phi}-L)\sin\theta \cos\psi &= I_1\dot{\theta}\sin\psi \\
(I_3\dot{\phi}-L)\cos\theta &= -I_3\dot{\psi}
\end{aligned} \tag{2.3.8}$$

Solving for $\dot{\theta}$, $\dot{\phi}$, and $\dot{\psi}$ (L is constant in the inertial frame)

$$\begin{aligned}
\dot{\theta} &= 0 \\
\dot{\phi} &= \frac{L}{I_1} \\
\dot{\psi} &= \cos\theta \left(\frac{L}{I_3} - \frac{L}{I_1}\right)
\end{aligned} \tag{2.3.9}$$

Integrating (2.3.9) yields

$$\begin{aligned}
\theta &= \text{const.} = \theta_o \\
\phi &= \frac{L}{I_1}t + \phi_o \\
\psi &= \cos\theta\, L\left[\frac{1}{I_3} - \frac{1}{I_1}\right] t + \psi_o
\end{aligned} \tag{2.3.10}$$

Equations (2.3.10) are the linearly time dependent Euler angles of the TP.

In section 2.2, the TP parameters were given as:

$$I_1 = I_2 = 1.25 \text{ slug ft}^2$$

$$I_3 = .04 \text{ slug ft}^2$$

$$\omega_r' \simeq \pi = \frac{L}{I_1} \sin\theta$$

and

$$\omega_3' \simeq \pi = \frac{L}{I_3} \cos\theta$$

$$\tan\theta = \frac{I_1}{I_3} \simeq 30$$

$$\text{or } \theta \simeq 88°$$

Therefore, since the highest roll rate expected was assumed, we conclude that the TP is tumbling in a plane perpendicular to the angular momentum vector.

2.4 TUMBLE PERIOD

Two independent methods for the determination of the TP tumble period are available. The period between successive sun pulses can be read more accurately and is used for the tumble-period measurement, with the period between pressure maxima providing confirmation of the results. The tumble period is measured with an error of less than 2 msec (~1 part in 500).

2.5 ROLL PERIOD

Each cycle of the tumble motion causes the sun sensor to generate an output which is a function of the TP roll position. The roll rate is determined by the following analysis of this information:

Let

ω = roll rate (deg/sec)

θ = roll position of TP

k = an integer (0,1,2,...)

n = number of 1/2 tumble periods

t = time

then

$$\omega = \frac{\pm\theta_{(n+2)} - \theta_n \pm k\ 360^\circ}{t_{(n+2)} - t_n}$$

where

$t_{(n+2)} - t_n$ is simply the tumble period.

The role rate, in deg/sec, is equal to the number of degrees the TP has apparently rolled in one tumble period ($\pm\theta_{n+2} - \theta_n$), plus the number of complete cycles it has rolled ($\pm k\ 360^\circ$), divided by the tumble period—the time between roll position data inputs, θ_{n+2} and θ_n. The plus or minus signs are a consequence of the uncertainty in roll direction.

In the TP application, since the tumble period is less than the roll period, k is 0 and the equation becomes $\pm\theta_{n+2} - \theta_n / t_{n+2} - t_n$. Any pair of sensor outputs provide a solution; therefore, successive solutions can be used to prove the assumption k = 0 and also to indicate the correct sign in $\pm\theta_{n+2}$.

2.6 ORIENTATION ANALYSIS (Velocity Vector Reference)

Figure 6 shows the coordinate system used for the determination of $\bar{L}$. It is a right cartesian-coordinate system in which the z axis is pointing at the sun.

The $\overline{TP}_1$, and $\overline{TP}_2$ vectors describe the position of the TP cylinder axis, the direction being that of the normal to the orifice of the pressure gauge. $\overline{TP}_1$ is the position of the TP at the time it is closest to the velocity vector, i.e., the time a maximum pressure reading is recorded. $\overline{TP}_2$ is the position of the TP at the time a sun pulse is received. $\overline{TP}_2$ is in the x-y plane since the sun sensor is perpendicular to the axis of the TP.

The angle γ_1 is the angle between $\overline{TP}_1$ and $\overline{TP}_2$. It is determined by measuring the time difference, Δt, between a peak pressure reading and a sun pulse. The angle γ_1 is then given by:

$$\gamma_1 = 360^\circ \times \frac{\Delta t}{\text{tumble period}} .$$

The angle γ_2 is the half angle of the cone, about the z axis, of all possible angular momentum vectors. This is determined by the following analysis:

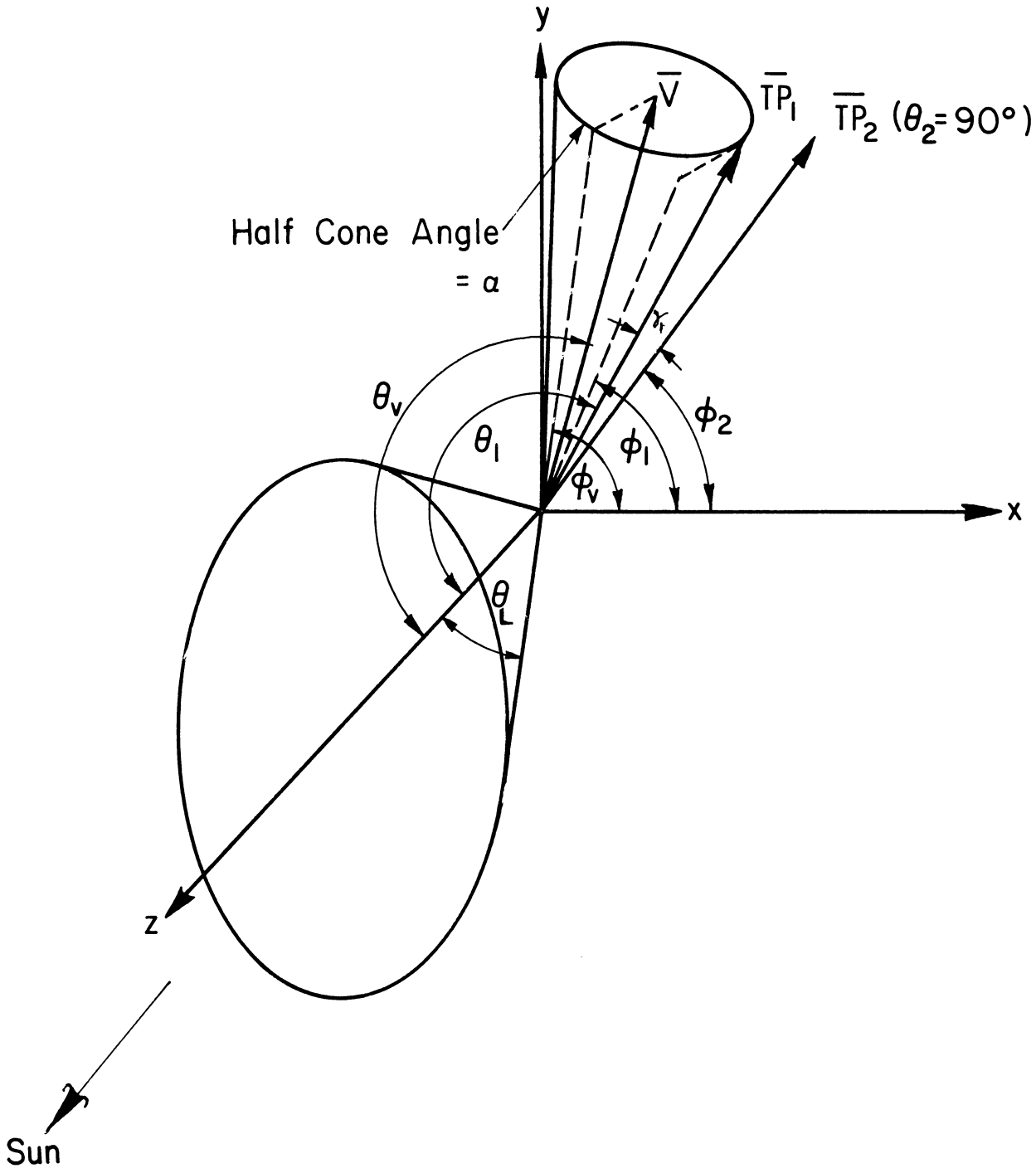

Fig. 6. Coordinates for TP orientation, velocity vector reference.

Let

t = time

n = number of 1/2 tumble periods

ω = roll rate

γ_2 = cone half angle of $\bar{L}$ from z axis

Θ = sun sensor roll position

Then, assuming that the roll rate is less than the tumble rate:

$$2\gamma_2 = \Theta_{n+1} - \Theta_n + \omega(t_{n+1}-t_n) \quad .$$

Once one knowns Θ_n and where the sun sensor has rolled to in half a tumble period, Θ_{n+1} can only be the received output for one plane of tumble with respect to the sun vector. γ_2 is the half angle of the cone of possible angular momentum vectors about z.

2.7 ORIENTATION EQUATIONS

Referring to Fig. 6 which shows the vectors to be determined, the equations to be solved are the following:

Assuming the TP is tumbling in a plane, we get:

$$\overline{TP}_1 \cdot \bar{L} = \overline{TP}_2 \cdot \bar{L} = 0. \qquad (2.7.1)$$

From our previous definiton of γ_1:

$$\overline{TP}_1 \cdot \overline{TP}_2 = \cos \gamma_1 \quad . \qquad (2.7.2)$$

Since the $\overline{TP}_1$ vector is tangent to the cone of minimum angle of attack, we can say:

$$\bar{L} \cdot \overline{TP}_1 \times \bar{V} = 0 \quad . \qquad (2.7.3)$$

The minimum angle of attack, α, is then given by:

$$\frac{\overline{TP}_1 \cdot \overline{V}}{|\overline{V}|} = \cos \alpha \qquad (2.7.4a)$$

or

$$\frac{\overline{L} \cdot \overline{V}}{|\overline{V}|} = \sin \alpha \, . \qquad (2.7.4b)$$

Assuming all vectors, except $\overline{V}$, are unit vectors.

Using typical spherical coordinates, Θ measured from the z axis and ϕ, the angle in the x-y plane, measured counterclockwise from the x axis, we can solve the above four equations for the unknown quantity ϕ_L, the ϕ position of $\overline{L}$. Θ_L is by definition equal to γ_2.

The solutions are:

$$\cos(\phi_1-\phi_2) = \left[\frac{A^2+\cos^2\gamma_1}{A^2+1}\right]^{1/2} \qquad (2.7.5)$$

where

$$A = \frac{\cos \gamma_1}{\cos \gamma_2}$$

$$\sin \Theta_1 = \frac{\cos \gamma_1}{\cos(\phi_1-\phi_2)} \qquad (2.7.6)$$

$$\phi_2-\phi_L = \pm \frac{\pi}{2} \qquad (2.7.7)$$

$$\sin(\phi_1-\phi_V) = \frac{BC \pm \sqrt{B^2-C^2+1}}{B^2+1} \, . \qquad (2.7.8a)$$

for $\phi_2-\phi_L = \frac{\pi}{2}$

$$\sin(\phi_1-\phi_V) = \frac{-BC \pm \sqrt{B^2-C^2+1}}{B^2+1} \qquad (2.7.8b)$$

for $\phi_2-\phi_L = -\frac{\pi}{2}$

where

$$B = \frac{\sin^2(\phi_1-\phi_2)+\cot^2\gamma_2}{\sin(\phi_1-\phi_2)\cos(\phi_1-\phi_2)}$$

$$C = \frac{\cot\gamma_2 \cot\Theta_V}{\sin(\phi_1-\phi_2)} .$$

The above equations yield eight solutions for ϕ_L.

If this analysis is carried out at two or more times during the flight, with data input from the sun sensor, only one of the eight solutions will yield the same ϕ_L each time. This then is the correct ϕ_L, and the angular momentum vector is known.

2.8 ORIENTATION ANALYSIS (Earth Normal Reference)

In this method, the output from an earth sensing instrument is used to determine the time when the TP is closest to the local earth normal vector, $\overline{N}$. The equations for this case are similar to those of the previous method (see Fig. 7).

Let $\overline{TP}_2$ = position of TP when a sun pulse is recorded

$\overline{TP}_3$ = position of TP when closest to $\overline{N}$ (earth sensor data)

$\overline{N}$ = Local normal to earth's surface

$\overline{L}$ = angular momentum vector

γ_3 = angle between $\overline{TP}_2$ and $\overline{TP}_3$ (minimum) (measured)

Θ_L = half angle of cone of possible angular momentum vectors (measured)

$$\overline{TP}_2 \cdot \overline{L} = \overline{TP}_3 \cdot \overline{L} = 0 \qquad (2.8.1)$$

$$\overline{TP}_2 \cdot \overline{TP}_3 = \cos\gamma_3 \qquad (2.8.2)$$

$$\overline{L} \cdot \overline{TP}_3 \times \overline{N} = 0 \qquad (2.8.3)$$

$$\frac{\overline{L}\cdot\overline{V}}{|\overline{V}|} = \sin\alpha \qquad (2.8.4)$$

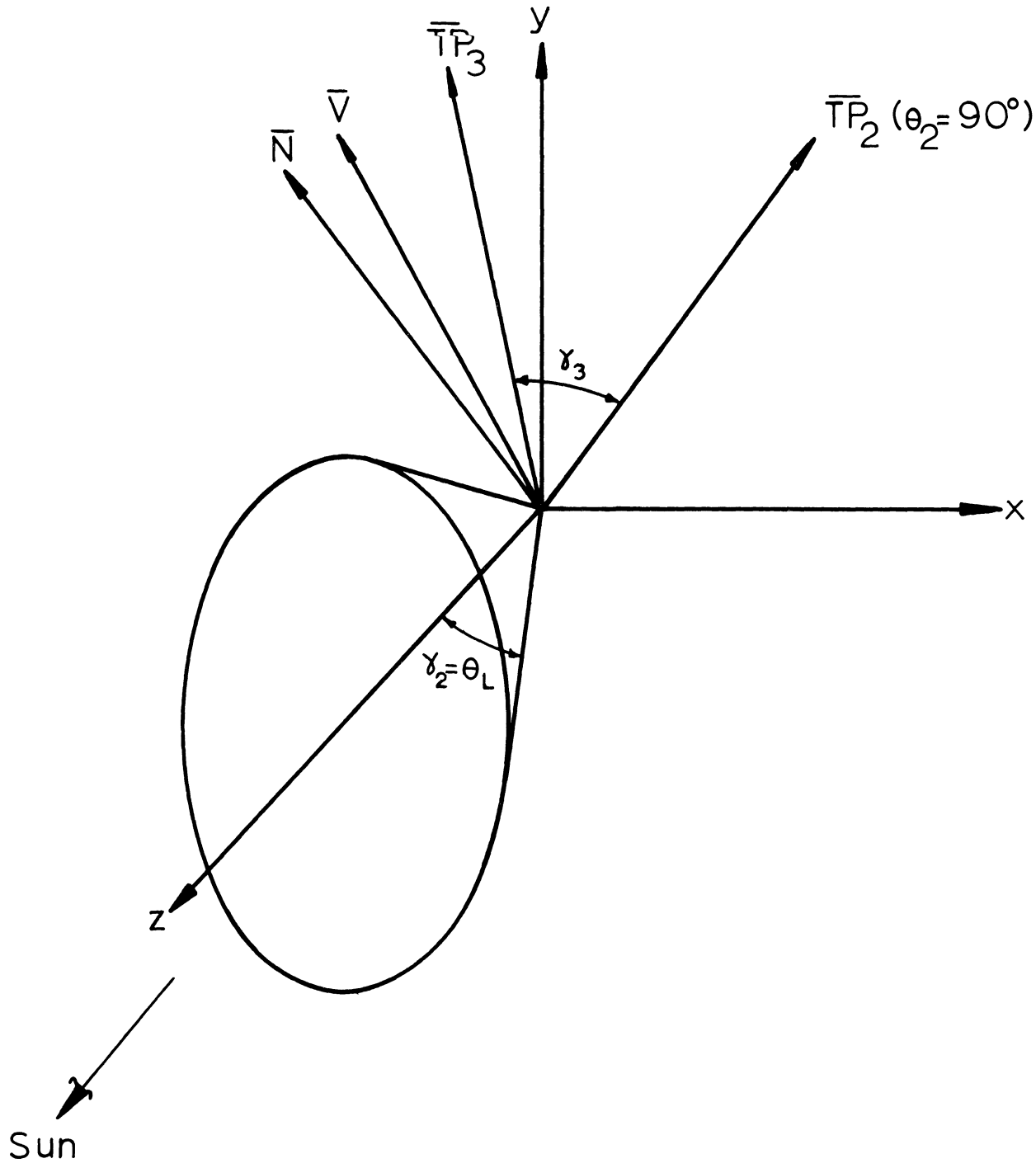

Fig. 7. Coordinates for TP orinetation, earth normal reference.

The solutions are:

$$\cos(\phi_3 - \phi_2) = \left[\frac{A'^2 + \cos^2 \gamma_3}{A'^2 + 1} \right]^{1/2} \tag{2.8.5}$$

where

$$A' = \frac{\cos \gamma_3}{\cos \theta_L}$$

$$\sin \theta_3 = \frac{\cos \gamma_3}{\cos(\phi_3 - \phi_2)} \tag{2.8.6}$$

$$\phi_2 - \phi_L = \pm \pi/2 \tag{2.8.7}$$

where, for $\phi_2 - \phi_L = \pi/2$

$$\sin(\phi_3 - \phi_N) = \frac{B'C' \pm \sqrt{B'^2 - C'^2 + 1}}{B'^2 + 1} \tag{2.8.8}$$

and for $\phi_2 - \phi_L = -\pi/2$

$$\sin(\phi_3 - \phi_N) = \frac{-B'C' \pm \sqrt{B'^2 - C'^2 + 1}}{B'^2 + 1} \tag{2.8.9}$$

where

$$B' = \frac{\sin^2(\phi_3 - \phi_2) + \cot^2 \theta_L}{\sin(\phi_3 - \phi_2)\cos(\phi_3 - \phi_2)}$$

$$C' = \frac{\cot \theta_L \cot \theta_N}{\sin(\phi_3 - \phi_2)}$$

As for the previous case (Sec. 2.7), the equations yield eight solutions for ϕ_L. An analysis at several points along the trajectory eliminates the ambiguity.

2.9 DIRECT METHOD OF OBTAINING α

Another method of finding α directly is discussed below. This method gives a more understandable physical picture of the TP's motion and yields α directly for each time sun sensor data are available.

Figure 8 shows the plane of tumble (shaded plane) and its relationship to the measured quantities, γ_1 and γ_2. The cone half angle $\overline{AD}$ is equal to $(\pi/2)-\gamma_2$. It is the cone to which all possible tumble planes must be tangent. $\overline{EB}$ is the angle γ_1, the angle measured between a sun-pulse and a peak-pressure measurement (at B). The circle about the sun vector of radius $\overline{AB}$ describes the locus of all possible positions of the TP when a peak-pressure measurement was received. The criterion for a solution is that the tumble plane must be tangent to the cone $\overline{AD}$ and must be tangent to a cone about the velocity vector (cone half angle $\overline{BC}$) at a point on the cricle of radius AB (Θ_1 of our previous analysis). The angle BC is by definition the minimum angle of attack α, to be solved for.

The problem then is to solve the spherical triangles for the angle BC = α in terms of the known quantities AB = Θ_1, BD = $(\pi/2)-\gamma_1$, AC = Θ_V, AD = $(\pi/2)-\gamma_2$ (see Fig. 9).

$$\cos \overline{AC} = \cos \overline{BC} \cos \overline{AB} + \sin \overline{BC} \sin \overline{AB} \cos(90°+\mu)$$

or

$$\cos \overline{AC} = \cos \overline{BC} \cos \overline{AB} - \sin \overline{BC} \sin \overline{AB} \sin \mu \qquad (2.9.1)$$

also

$$\cos \overline{AB} = \cos \overline{AD} \cos \overline{BD} + \sin \overline{AD} \sin \overline{BD} \cos 90°$$

or

$$\cos \overline{AB} = \cos \overline{AD} \cos \overline{BD} \, . \qquad (2.9.2)$$

Now, from the sine law:

$$\frac{\sin \overline{AB}}{\sin \frac{\pi}{2}} = \frac{\sin \overline{AD}}{\sin \mu}$$

or

$$\sin \overline{AB} = \frac{\sin \overline{AD}}{\sin \mu} \, . \qquad (2.9.3)$$

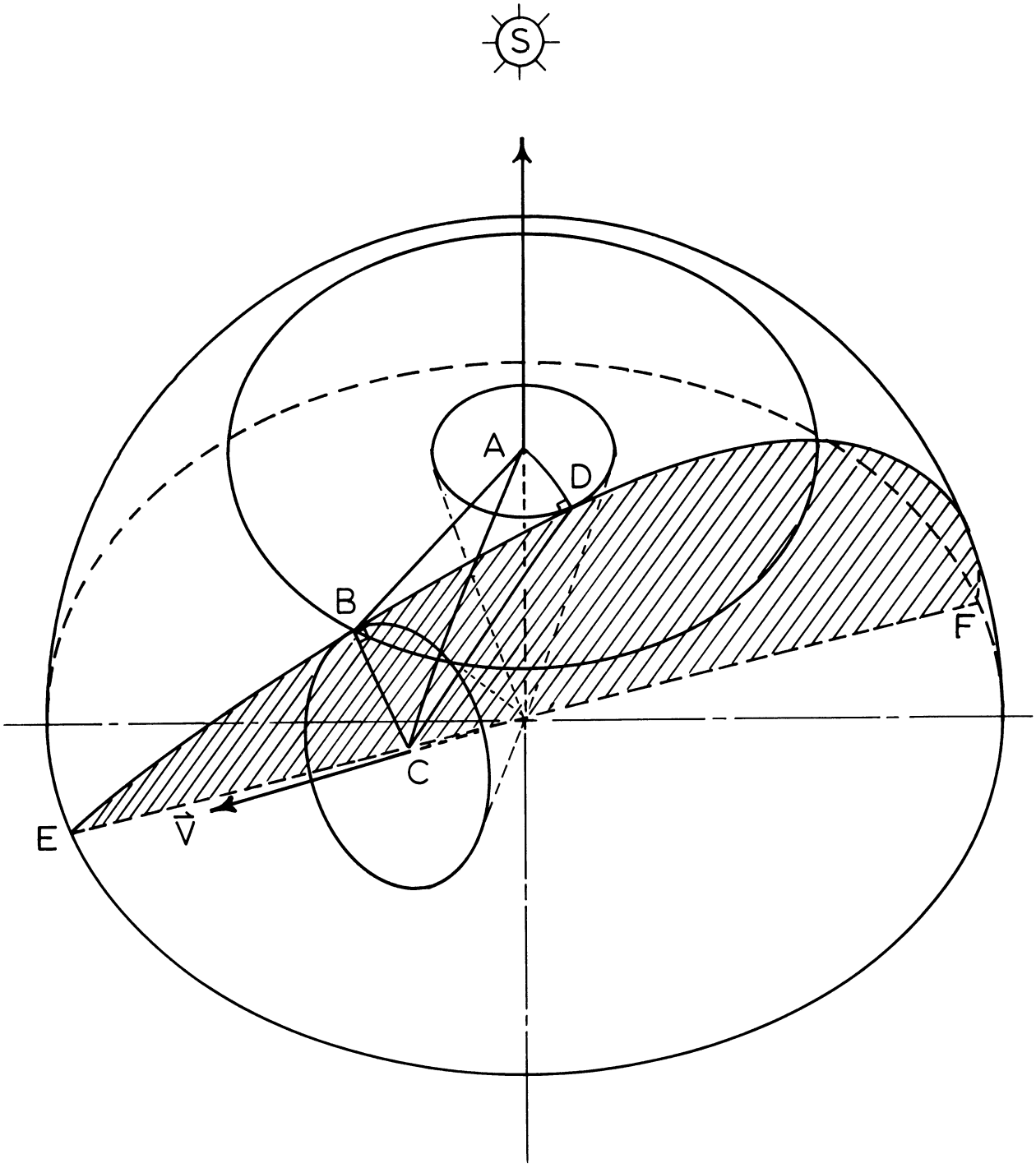

Fig. 8. Coordinates for direct method of angle of attack analysis.

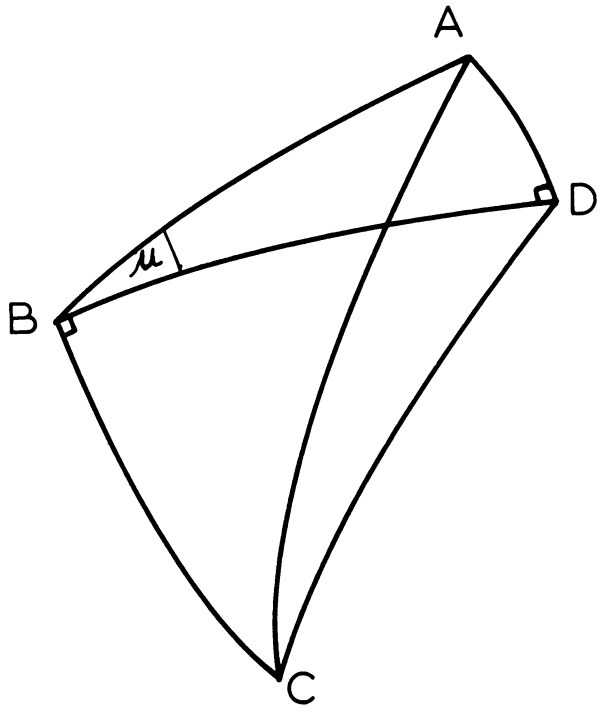

Fig. 9. Spherical triangles of Fig. 8.

Substituting Eqs. (2.9.2) and (2.9.3) into Eq. (2.9.1), we get:

$$\cos \overline{AC} = \cos \overline{BC} \cos \overline{AD} \cos \overline{BD} - \sin \overline{BC} \sin \overline{AD} . \qquad (2.9.4)$$

Rearranging

$$\cos \overline{AC} - \cos \overline{BC} \cos \overline{AD} \cos \overline{BD} = -\sqrt{1-\cos^2 \overline{BC}} \sin \overline{AD}.$$

Squaring both sides

$$\cos^2 \overline{AC} + \cos^2 \overline{BC} \cos^2 \overline{AD} \cos^2 \overline{BD} - 2 \cos \overline{AC} \cos \overline{BC} \cos \overline{AD} \cos \overline{BD}$$

$$= \sin^2 \overline{AD} - \cos^2 \overline{BC} \sin^2 \overline{AD} .$$

Rearranging

$$\cos^2 \overline{BC}[\cos^2 \overline{AD} \cos^2 \overline{BD} + \sin^2 \overline{AD}] - 2 \cos \overline{BC}(\cos \overline{AC} \cos \overline{AD} \cos \overline{BD})$$

$$+ (\cos^2 \overline{AC} - \sin^2 \overline{AD}) = 0 .$$

Let

$$\ell = \cos^2 \overline{AD} \cos^2 \overline{BD} + \sin^2 \overline{AD} = \cos^2\left(\frac{\pi}{2} - \gamma_2\right) \cos^2\left(\frac{\pi}{2} - \gamma_1\right) + \sin^2\left(\frac{\pi}{2} - \gamma_2\right)$$

$$m = \cos \overline{AC} \cos \overline{AD} \cos \overline{BD} = \cos \Theta_V \cos\left(\frac{\pi}{2} - \gamma_2\right) \cos\left(\frac{\pi}{2} - \gamma_1\right)$$

$$n = \cos^2 \overline{AC} - \sin^2 \overline{AD} = \cos^2 \Theta_V - \sin^2\left(\frac{\pi}{2} - \gamma_2\right)$$

$$\ell \cos^2 \overline{BC} - 2m \cos \overline{BC} + n = 0$$

and

$$\cos BC = \frac{m \pm \sqrt{m^2 - \ell n}}{\ell} . \qquad (2.9.5)$$

This analysis was carried out with the assumption that the position of the TP at minimum angle of attack was describable in the top hemisphere of the sun coordinate system shown in Fig. 8. If the TP is positioned on the bottom hemisphere [$\overline{AB} > (\pi/2)$] then the angle $\overline{BD}$ is [$(\pi/2)+\gamma_1$)].

For $\overline{AB} < \frac{\pi}{2}$, $\gamma_2 < \frac{\pi}{2}$

$$\ell = \sin^2\gamma_2 \sin^2\gamma_1 + \cos^2\gamma_2$$

$$m = \cos \Theta_V \sin \gamma_2 \sin \gamma_1$$

$$n = \cos^2\Theta_V - \cos^2\gamma_2$$

and for $\overline{AB} > \frac{\pi}{2}$, $\gamma_2 < \frac{\pi}{2}$

$$\ell = \sin^2\gamma_2 \sin^2\gamma_1 + \cos^2\gamma_2$$

$$m = - \cos \Theta_V \sin \gamma_2 \sin \gamma_1$$

$$n = \cos^2\Theta_V - \cos^2\gamma_2$$

where

$$\cos \alpha = \frac{m \pm \sqrt{m^2 - \ell n}}{\ell} \quad . \tag{2.9.6}$$

2.10 COMPUTER ANALYSIS

The orientation analysis described in Sections 2.5 and 2.6 have been programmed for digital computer solutions. The program instructs the computer to produce a theoretical trajectory, matched to radar data, with velocity components in both earth fixed and sun fixed coordinates. This trajectory is then used to obtain the eight solutions for each of two analysis points. The two groups of solutions are compared, and the correct angular momentum vector is selected and used to determine the minimum angle of attack versus flight time. Other parameters obtained from the results of the solution are shown in Fig. 10.

2.11 ATMOSPHERIC WIND

The use of the two orientation analyses described in Sections 2.4 through 2.6 permits a determination of the component of horizontal atmospheric wind in the plane of tumble of the TP. Since the velocity vector reference method determines the motion and, hence, angle of attack of the TP, with respect to the atmosphere and the sun, and the earth reference method determines the

MOMENTUM VECTOR DETERMINATION

TIME 141.000 GAMMA1 36.400 THETA1 100.000

LX	LY	LZ	PHIL	THETAL	PHI1-PHI2	PHI1-PHIV
-.73152	-.68039	.04408	133.456	37.300	30.390	37.347
.26239	-.93260	.24780	-107.325	37.300	-30.390	37.347
.10034	-.99357	.05253	-132.194	37.300	-30.390	12.478
-.81658	-.52640	.23685	108.587	37.300	30.390	12.478
.79540	.39315	-.46127	-96.368	142.700	30.390	-12.478
.12662	.98888	.07799	22.851	142.700	-30.390	-12.478
.37488	.91945	.11866	-2.019	142.700	-30.390	-37.347
.67206	.30624	-.67420	-121.238	142.700	30.390	-37.347

TIME 335.500 GAMMA1 57.300 THETA1 80.000

LX	LY	LZ	PHIL	THETAL	PHI1-PHI2	PHI1-PHIV
.37540	.91924	.11864	-2.071	142.700	51.095	19.536
-.27627	.92099	-.27467	-284.261	142.700	-51.095	19.536
-.13343	.98766	-.08201	-307.966	142.700	-51.095	-4.170
.59018	.80448	.06701	-25.777	142.700	51.095	-4.170
-.51955	-.84914	-.09498	-197.437	37.300	51.095	4.170
.19248	-.97051	.14513	-119.627	37.300	-51.095	4.170
.00469	-.59987	-.01562	-143.332	37.300	-51.095	-19.536
-.70023	-.71385	.00999	-221.143	37.300	51.095	-19.536

THE ''CORRECT'' MOMENTUM VECTOR IS .37488 .91945 .11866

68° 23° 83°

TIME	ALTITUDE	RANGE	POSITION DEGREES	INERTIAL VELOCITY FEET	VELOCITY WRT EARTH FEET	FIXED VEL FEET	AZIMUTH DEGREES	ELEVATION DEGREES	ALPHA
SEC	FEET METERS GEOPCT METER	FEET METERS	LATITUDE LONGITUDE	TOTAL HORIZONTAL VERTICAL	TOTAL HORIZONTAL VERTICAL	TOTAL HORIZONTAL VERTICAL	TOTAL HORIZONTAL VERTICAL	X Y Z	INERTIAL WRT EARTH	INERTIAL WRT EARTH	DEGREES RADIANS COSINE
393	214390	383089	37.08	5372	1638	5046	1538	667	112.32	-66.31	11.850
	65346	116766	-74.57	2158	658	1123	342	-761	136.86	-77.14	.207
	64682			-4920	-1500	-4920	-1500	-4944			.9787

motion with respect to the earth and sun, any differences between the two methods larger than the expected error must be due to atmospheric motion. Therefore, the quantity determined is an apparent difference in minimum angle of attack, $\Delta\alpha$. Although true wind velocity determination depends upon α_o, the minimum angle of attack, and other data input magnitudes, a theoretical plot of the horizontal wind velocity component in the plane of tumble versus altitude for a typical Nike-Tomahawk trajectory is given in Fig. 11.

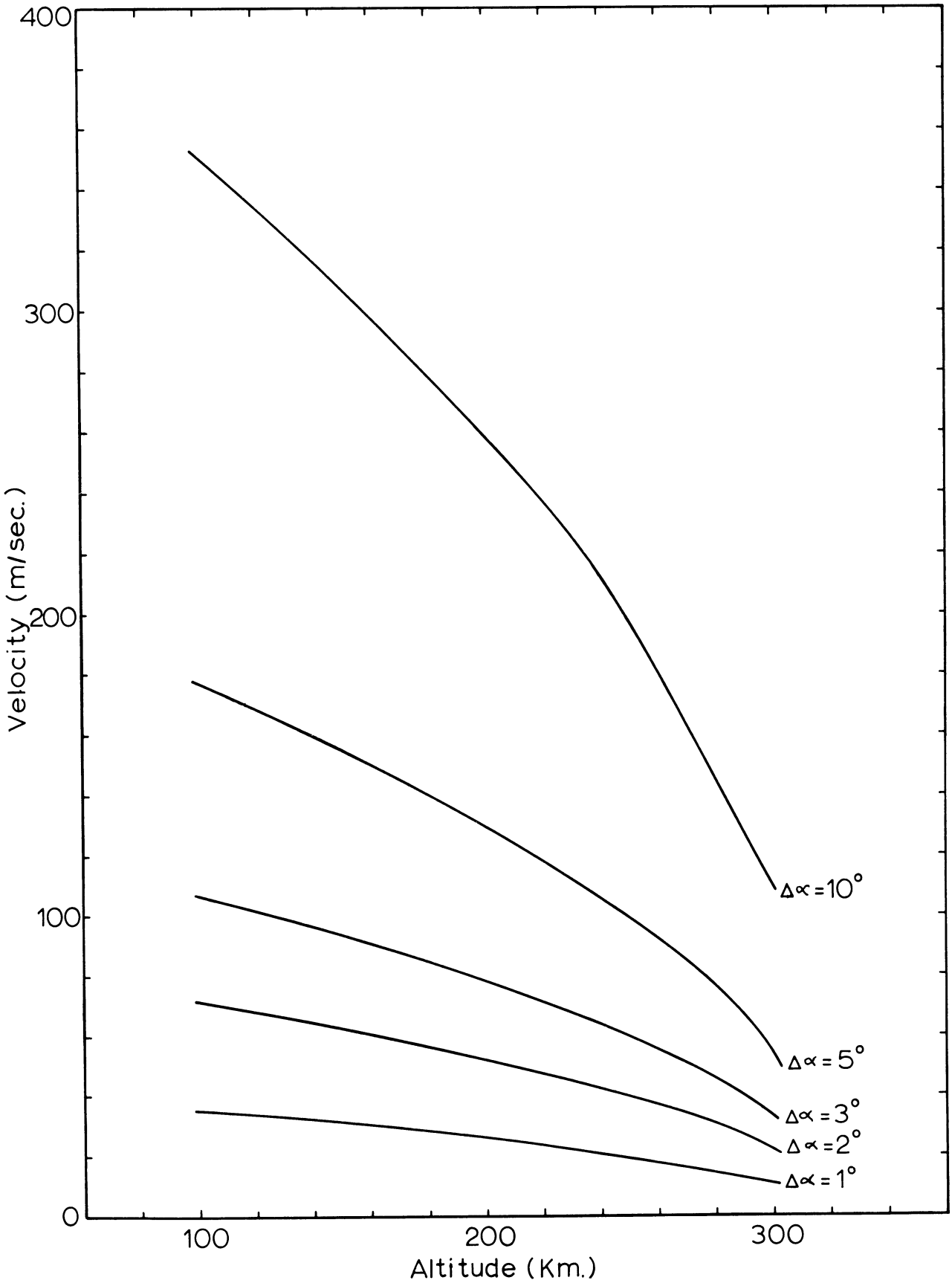

Fig. 11. Horizontal component of wind velocity in the plane of tumble vs. altitude for various $\Delta\alpha$.

3. DATA REDUCTION

3.1 N_2 DENSITY VS. ALTITUDE—DATA ANALYSIS

The pressure relationship across the orifice of a pressure gauge mounted within a moving, rotating body in a free-molecular-flow region in a planetary atmosphere, is given by the thermal transpiration equation as modified by drift velocity considerations.[3]

From Ref. 3

$$\frac{P_i}{P_o} = \sqrt{T_i/T_o}\, f(s) \qquad (3.1.1)$$

where

$$f(s) = e^{-s^2} + \sqrt{\pi}s(1+\text{erf}s)$$

$s = V \cos \beta/u$

$u = \sqrt{2kT/m}$

P = pressure

T = temperature

V = vehicle velocity

β = angle between the normal to the pressure-gauge orifice and the velocity vector

u = most probable thermal velocity for molecules of mass m

i = subscript denoting quantities inside the pressure gauge

o = subscript denoting quantities outside the pressure gauge

For the TP experiment, the pressure gauge is tumbling in a plane which is at an angle α (minimum angle) from the velocity vector. Considering the maximum change in pressure during one tumble period:

$$P_{i_{max}} - P_{i_{min}} = P_o\sqrt{T_i/T_o}\ [f(s)-f(-s)] \qquad (3.1.2)$$

since

$$f(+s) - f(-s) = \sqrt{\pi}\, s[\mathrm{erf}(s)-\mathrm{erf}(-s)] = 2\sqrt{\pi}\, s.$$

We get:

$$P_{i_{max}} - P_{i_{min}} = 2P_o \sqrt{\pi}\, s \sqrt{T_i/T_o} = \Delta P_i \,. \qquad (3.1.3)$$

From the ideal gas law:

$$P_o = \rho_o R T_o$$

we get:

$$\Delta P_i = 2\sqrt{\pi}\, R\rho_o \sqrt{T_i T_o}\; s \,.$$

Which, for ambient N_2 density, is:

$$\rho_o = \frac{\Delta P_i}{2\sqrt{\pi}\, R\sqrt{T_i T_o}\, \dfrac{V \cos \alpha}{u_o}} \qquad (3.1.4)$$

substituting $u = \sqrt{2kT/m}$, and rearranging yields:

$$\rho_o = \frac{\Delta P_i}{\sqrt{\pi}\, u_i\, V \cos \alpha} \quad \text{(see Ref. 4)} \,. \qquad (3.1.5)$$

In terms of number density:

$$n_{N_{2o}}\, m_{N_2} = \frac{kT_i \Delta n_{N_{2i}}}{\sqrt{\pi}\, U_i V \cos_\alpha}$$

or

$$n_{N_{2o}} = \frac{\Delta n_{N_{2i}}\, U_{N_{2i}}}{2\sqrt{\pi}\, V \cos_\alpha} \qquad (3.1.6)$$

Figure 12 gives typical values for $N_2 P_{i_{max}}$, $P_{i_{min}}$, and P_o for a typical Nike-Tomahawk trajectory.

3.1a O_2, O DENSITY VS. ALTITUDE—DATA ANALYSIS

Omagatron O_2 measurement—total recombination inside gauge assumed for $O \rightarrow O_2$.

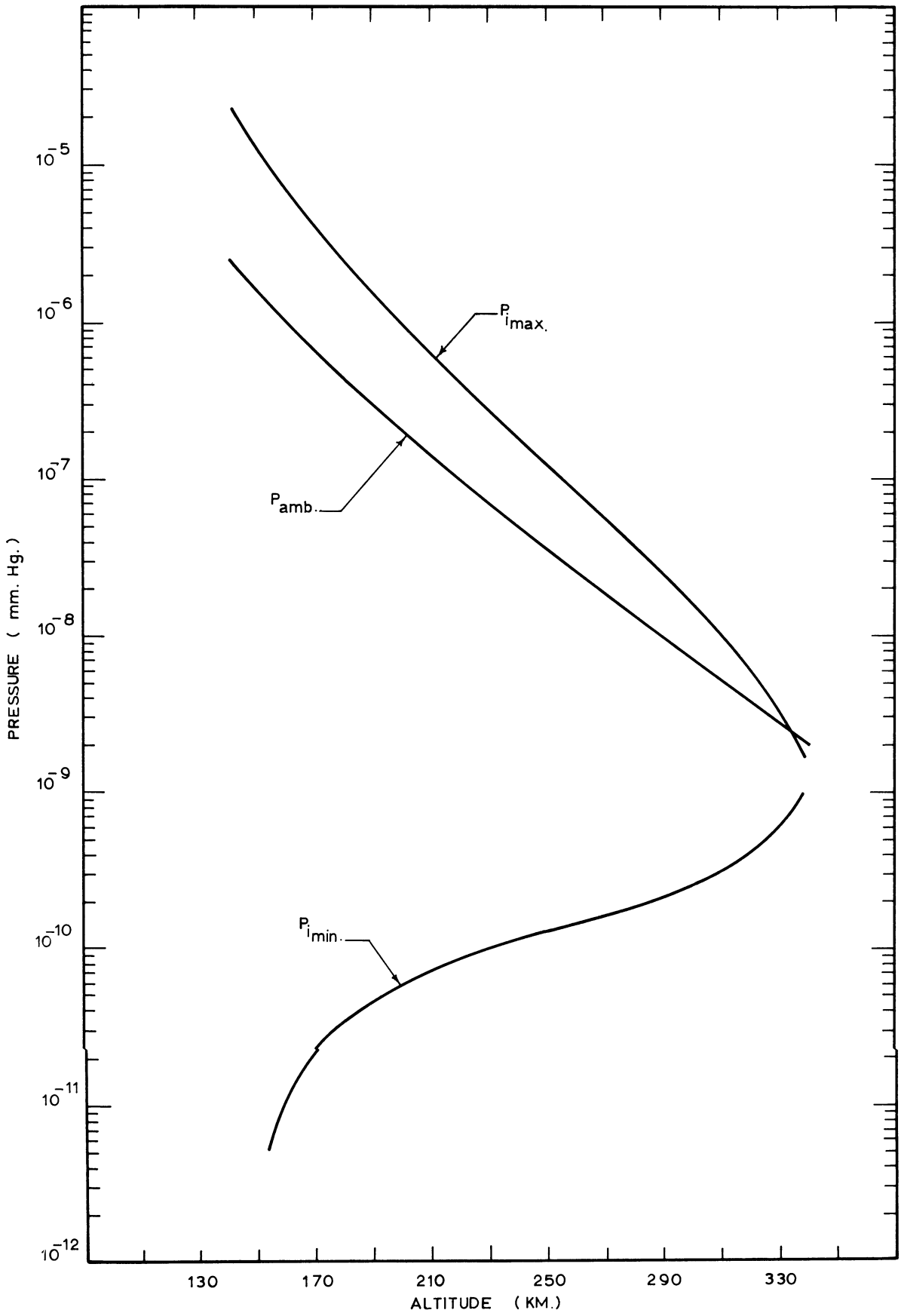

Fig. 12. N_2 $P_{i_{max}}$, $P_{i_{min}}$ and P_a vs. altitude for Nike-Tomahawk trajectory.

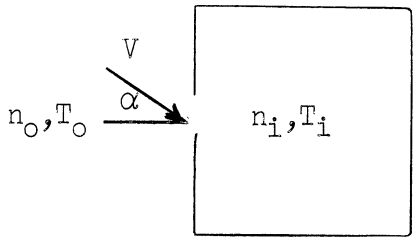

For equilibrium flow at orifice:

$$U_{o_{2_i}} \; n_{o_{2_i}} = U_{o_{2_o}} \; n_{o_{2_o}} \; f(S_{o_2}) + 1/2 \; n_{o_o} U_{o_o} f(S_o) \qquad (3.1.7)$$

where U = most probable thermal speed

$$= \sqrt{\frac{2kT}{m}}$$

Substituting the temperature and mass dependent expression for $U_{o_{2_i}}$ and dividing the right hand part of the equation -

$$n_{o_{2_i}} = \sqrt{\frac{T_o}{T_i}} \; n_{o_{2_o}} \; f(S_{o_2}) + 1/2 \sqrt{\frac{M_{o_2}}{M_o}} \sqrt{\frac{T_o}{T_i}} \; n_{o_o} \; f(S_o) \qquad (3.1.8)$$

$$\Delta n_{o_{2_i}} = \frac{2\sqrt{\pi} \; V \cos\alpha}{U_{o_{2_i}}} \; [n_{o_{2_o}} + 1/2 n_{o_o}]$$

or

$$n_{o_{2_o}} + 1/2 n_{o_o} = \frac{\Delta n_{o_{2_i}} \; U_{o_{2_i}} \equiv f(\Delta n_{o_{2_i}})}{2\sqrt{\pi} \; V \cos_\alpha} \qquad (3.1.9)$$

Assuming diffusion equilibrium, the hydrostatic equation for each species can be written:

mult. by 1/2

$$kT_o \frac{dn_o}{dh} + k \frac{dT_o}{dh} \; n_o = - 1/2 M_{o_2} \; g n_o$$

and

$$kT_o \frac{dno_2}{dh} + k \frac{dT_o}{dh} \; n_{o_2} = -M_{o_2} \; g n_{o_2}$$

add

$$kT_o \frac{df(\Delta n)}{dh} + k \frac{dT_o}{dh} f(\Delta n) = -M_{o_2} g(1/4n_o + n_{o_2}) \qquad (3.1.10)$$

or

$$1/4n_{o_o} + n_{o_{2_o}} = -\frac{k}{M_{o_2} g} \left[T_o \frac{df(\Delta n)}{dh} + \frac{dT_o}{dh} f(\Delta n)\right] \equiv -g(\Delta n) \qquad (3.1.11)$$

Using equation for g(ΔN) and f(ΔN) (3.1.9) and (3.1.11) we get:

$$n_{o_{2_o}} = -2g(\Delta n) - f(\Delta n) \qquad (3.1.12)$$

$$n_o = 4\,[f(\Delta n) + g(\Delta n)]$$

and

$$\frac{n_o}{n_{o_2}} = -\frac{4[g(\Delta n) + f(\Delta n)]}{2g(\Delta n) + f(\Delta n)} \qquad (3.1.13)$$

also

$$g(\Delta n) = -\frac{\left[\frac{n_o}{n_{o_2}} + 4\right]}{\left[2\frac{n_o}{n_{o_2}} + 4\right]} f(\Delta n) \qquad (3.1.14)$$

$\frac{n_o}{n_{o_2}}$	$g(\Delta n)$
0	$-f(\Delta n)$
0.5	$-.900f(\Delta n)$
1.0	$-.833f(\Delta n)$
2.0	$-.750f(\Delta n)$
∞	$-.500f(\Delta n)$

Therefore, the ambient number densities of O_2 and O are separable and determinable from the O_2 density measurement within a gauge open to the atmosphere through a knife edge orifice. The validity of the assumption that total recombination of O into O_2 occurs within the gauge is questionable. However, measurements of O during any typical flight would yield the data required to determine what fraction has recombined into O_2, and similar equations can easily be derived.

3.2 AMBIENT NEUTRAL TEMPERATURE VS. ALTITUDE—SCALE HEIGHT METHOD

The determination of ambient gas temperature from pressure measurements in a moving and tumbling pressure gauge can be accomplished by two independent methods. One method is the determination of a scale height for the ambient gas; the other uses the "velocity scan" technique,[3] which determines the relationship between the vehicle velocity, a known parameter, and the most probable thermal velocity of the ambient particles, a quantity proportional to the square root of the temperature.

For the first method, we assume an atmosphere at equilibrium such that the hydrostatic equation holds:

$$\frac{dP}{dh} = - \rho g . \tag{3.2.1}$$

Also, we assume the ideal gas law is valid:

$$P = \rho RT . \tag{3.2.2}$$

Differentiating Eq. (3.2.2) with respect to altitude, we get:

$$\frac{dP}{dh} = RT \frac{d\rho}{dh} + \rho R \frac{dT}{dh} . \tag{3.2.3}$$

Substituting Eq. (3.2.3) into Eq. (3.2.1):

$$RT \frac{d\rho}{dh} + \rho g + \rho R \frac{dT}{dh} = 0$$

or

$$RT \frac{d\rho}{dh} + \rho \left(g + R \frac{dT}{dh} \right) = 0 . \tag{3.2.4}$$

For the TP experiment, the expression for ambient density was derived previously:

$$\rho = \frac{\Delta P_i}{U_i \sqrt{\pi}\, V \cos \alpha} . \tag{3.2.5}$$

Now

$$\frac{d\rho}{dh} = \frac{1}{U_i \sqrt{\pi}\, V \cos \alpha} \left[\frac{d\Delta P_i}{dh} - \frac{\Delta P_i}{V} \frac{dV}{dh} + \tan \alpha\, \Delta P_i \frac{d\alpha}{dh} \right] . \tag{3.2.6}$$

Substituting Eqs. (3.2.5) and (3.2.6) into Eq. (3.2.4) and cancelling common terms

$$T = -\left(\frac{g}{R} + \frac{dT}{dh}\right) \frac{\Delta P_i}{\frac{d\Delta P_i}{dh} - \frac{\Delta P_i}{V}\frac{dV}{dh} + \tan\alpha\, \Delta P_i \frac{d\alpha}{dh}} \qquad (3.2.7)$$

This expression relates the ambient temperature to the basic pressure measurement and trajectory information. To change the equation to a form more suitable for data reduction, we multiply the numerator and denominator by $V_z = dh/dt$,

$$T = -\left(\frac{g}{R} + \frac{dT}{dh}\right) \frac{\Delta P_i\, V_z}{\frac{d\Delta P_i}{dt} - \frac{\Delta P_i}{V}\frac{dV}{dt} + \tan\alpha\, \Delta P_i \frac{d\alpha}{dt}} \quad . \qquad (3.2.8)$$

Equation (3.2.8) allows one to reduce much of the data, in terms of flight time, from the original telemetry records, eliminating trajectory information requirements until final analysis.

Returning to Eqs. (3.2.1) and (3.2.2), we see that Eq. (3.2.1) can be expressed as:

$$P_1 - P_2 = \int_{h_2}^{h_1} \rho g\, dh \quad . \qquad (3.2.9)$$

Where P_1 is the ambient pressure at altitude h_1 and P_2 is the ambient pressure at altitude h_2.

From Eq. (3.2.2), we can express ambient temperature as:

$$T = P/\rho R \quad .$$

Therefore,

$$T_1 = \frac{\int_{h_2}^{h_1} \rho g\, dh + P_2}{\rho_1 R} \qquad (3.2.10)$$

P_2 can be determined by

$$T_2 = P_2/\rho_2 R \quad .$$

Where T_2 is obtained from the data using Eq. (3.2.8).

Equations (3.2.8) and (3.2.10) are both valid for the assumption of Eqs. (3.2.1) and (3.2.2). Both equations have been used for data reduction and excellent agreement in the results is obtained.

Another technique for temperature determination which is independent of Eq. (3.2.1) is discussed in the following section

3.3 AMBIENT TEMPERATURE VS. ALTITUDE—VELOCITY SCAN METHOD

The velocity scan method for determining ambient temperature has been derived previously and is reported in Ref. 3. For this the thermal transpiration equation is used.

$$\frac{P_i}{P_o} = \sqrt{T_i/T_o}\ f(s) \qquad (3.3.1)$$

Since the TP is tumbling in a plane whose angle from the velocity vector is α, the angle of attack, β, for any given pressure reading is:

$$\cos\beta = \cos\alpha \cos\Theta$$

where Θ is the rotation angle in degrees in the plane of tumble. Θ is zero when $\beta = \alpha$, and a peak pressure reading is obtained. For any given tumble period, it can be assumed that the ambient temperature is constant, therefore, the ratio of (3.3.1) at β_1, to (3.3.1) at β_2 yields:

$$(P_{i_{\beta_1}}/P_{i_{\beta_2}}) = f(s_{\beta_1})/f(s_{\beta_2}) \qquad (3.3.2)$$

where

$$f(s) = e^{-s^2} + \sqrt{\pi}\ s(1+\mathrm{erf}s)$$

$$s_1 = V \cos\alpha \cos\Theta_1/u_o$$

$$u_o = \sqrt{2kT_o/m}$$

As is known:[3]

$$\lim_{s\to\infty} f(s) = 2\sqrt{\pi}\ s.$$

Therefore, for high S ($s > 2$), the linearity of $f(s)$ causes:

$$P_{i_{\beta_1}}/P_{i_{\beta_2}} = \cos\Theta_1/\cos\Theta_2.$$

However, if the 90° point ($\theta = 90°$), for example, and the peak pressure point ($\theta = 0°$) are chosen for the pressure reading.

$$P_{i_\alpha}/P_{i_{90°}} = f(S_\alpha) \quad . \tag{3.3.3}$$

From this ratio, an S can be determined. The ambient temperature is then given by:

$$T_o = \frac{m}{2k} \left(\frac{V \cos \alpha}{s_\alpha} \right)^2 \tag{3.3.4}$$

where V, s, α, m and k are known quantities.

It will briefly be noted here that the errors involved in reducing data from Eq. (3.3.4) above become quite large for high vehicle velocities, since all the temperature information is contained at points on the pressure curve near $\theta = 90°$, where S is small (Fig. 13). Also, the inherent inaccuracy of a linear amplifier at low outputs, compared to full scale outputs, causes errors in $P_{90°}$ that appear to approach and even exceed 100% especially when background pressure effects are also present. A thorough error analysis of this technique has been initiated and will be reported separately when completed. Therefore, the data presented in a later section was reduced using the previous method (scale height). In either case, assuming the gauge has a linear pressure-current characteristic, a systematic calibration error does not cause an error in the computed ambient temperature, since only ratios of the measured pressures are involved in the expressions used.

3.4 ELECTRON TEMPERATURE AND DENSITY--DATA ANALYSIS

The equations for the current collected by a stationary cylindrical probe immersed in a plasma were derived by Mott-Smith, and Langmuir (1926).[6] An extension of this work to moving cylindrical probes was carried out recently by Kanal (1964).[7] The thermal velocity of the electrons is very large in comparison with typical spacecraft velocities, thus for electron current calculations the probe can in effect be considered stationary. The Debye length corresponding to typical F-region conditions is of the order of 1 cm. The dimension of the sheath which surrounds the collector is of the order of the Debye length and since the radius of the collector used in these experiments is only 0.027 cm, a large sheath radius to probe radius ratio results. The retarded and accelerated current equations under these conditions are given by (3.4.1) and (3.4.2), respectively.

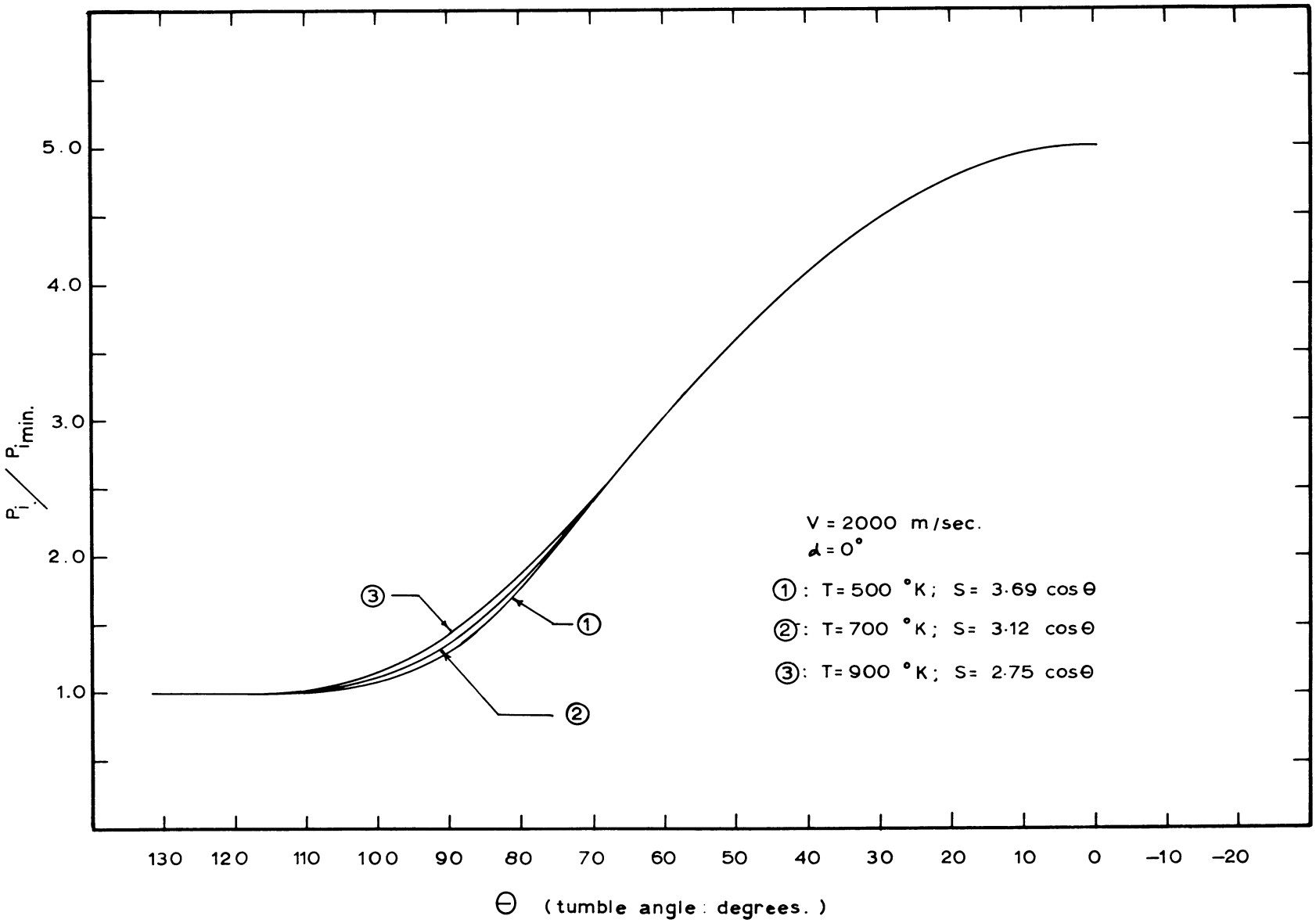

Fig. 13. Temperature effect on P_i vs. Θ.

$$I_r = \left(\frac{kT_e}{2\pi m_e}\right)^{1/2} N_e q\, A \exp(V_o) \qquad (3.4.1)$$

$$I_a = \left(\frac{kT_e}{2\pi m_e}\right)^{1/2} N_e qA \left[\frac{2}{\pi^{1/2}}\, V_o^{1/2} + \exp(V_o)\operatorname{erfc}(V_o^{1/2})\right] \qquad (3.4.2)$$

where:

k = Boltzmann's constant

T_e = temperature

m_e = mass

N = number density

q = magnitude of electronic charge

A = collector area

$V_o = \dfrac{qV_{pp}}{kT_e}$

V_{pp} = potential difference between the probe and the ambient plasma

$= V_{ap} + V_R$

V_{ap} = applied voltage

V_R = potential of the Thermosphere Probe with respect to the plasma

$\operatorname{erfc}(x)$ = complimentary error function

$$= 1 - \frac{2}{\pi^{1/2}} \int_o^x \exp[-\beta^2]\, d\beta$$

Let Eq. (3.4.1) be rewritten in the following manner:

$$I_r = \left(\frac{kT_e}{2\pi m_e}\right)^{1/2} N_e qA \exp\left[\frac{qV_{ap}}{kT_e}\right] \exp\left[\frac{qV_R}{kT_e}\right] \qquad (3.4.3)$$

Taking the natural logarithm of Eq. (3.4.3) one obtains:

$$\ell n(I_r) = \ell n \left[\left(\frac{kT_e}{2\pi m_e} \right)^{1/2} N_e q A \right] + \frac{qV_{ap}}{kT_e} + \frac{qV_R}{kT_e} \qquad (3.4.4)$$

The sawtooth voltage applied to the probe is made to vary from about -0.5V to approximately +5.0V at a rate of 4-5 c/s. This rate is sufficiently high to justify the assumption that the ambient parameters (density and temperature) remain constant during one sweep. Thus, assuming that the equilibrium potential of the TP as well as the atmospheric parameters remain constant during a sweep, differentiation of Eq. (3.4.4) with respect to V_{ap} yields:

$$\frac{d[\ell\, n(I_r)]}{d[V_{ap}]} = \frac{q}{kT_e} = \frac{11,600}{T_e} \qquad (3.4.5)$$

Therefore if $\ell\, n(I_r)$ is plotted versus V_{ap} a straight line results if the velocity distribution of the electrons is Maxwellian. The slope of this curve directly yields the electron temperature T_e. Such a curve obtained from typical experimental results is shown in Fig. 14.

The retarded current equation [Eq.(3.4.1)] shows an exponential relation between the collected current and the voltage, whereas the equation for accelerated current [Eq. (3.4.2)] shows a strong departure from such behavior. Therefore, ideally the plot of the electron current as a function of the applied voltage on a semilog paper will result in a straight line for positive applied voltages, up to the point where the cylinder reaches the plasma potential. The applied potential corresponding to this breakpoint is then equal in magnitude and opposite in sign to the equilibrium reference (TP) potential. Such a curve, constructed from typical experimental points was shown in Fig. 14. The establishment of this breakpoint, therefore, yields the equilibrium potential of the TP body. The electron current collected by a probe at the plasma potential, referred to as the random current, is given by Eq. (3.4.6).

$$I_{er} = \left(\frac{kT_e}{2\pi m_e} \right)^{1/2} N_e q A \qquad (3.4.6)$$

Once the equilibrium potential (V_R) is determined by this "breakpoint method" the value of the random electron current can easily by found. Using the electron temperatures derived from the slope of retarded characteristics, the ambient electron densities are calculated from the random electron current.

Equation (3.4.2) for the accelerated current contains two unknowns: the ambient electron density and the reference potential. The fact that these unknowns and the other parameters in Eq. (3.4.2) can be considered constant during one sweep, as discussed above, leads to another technique

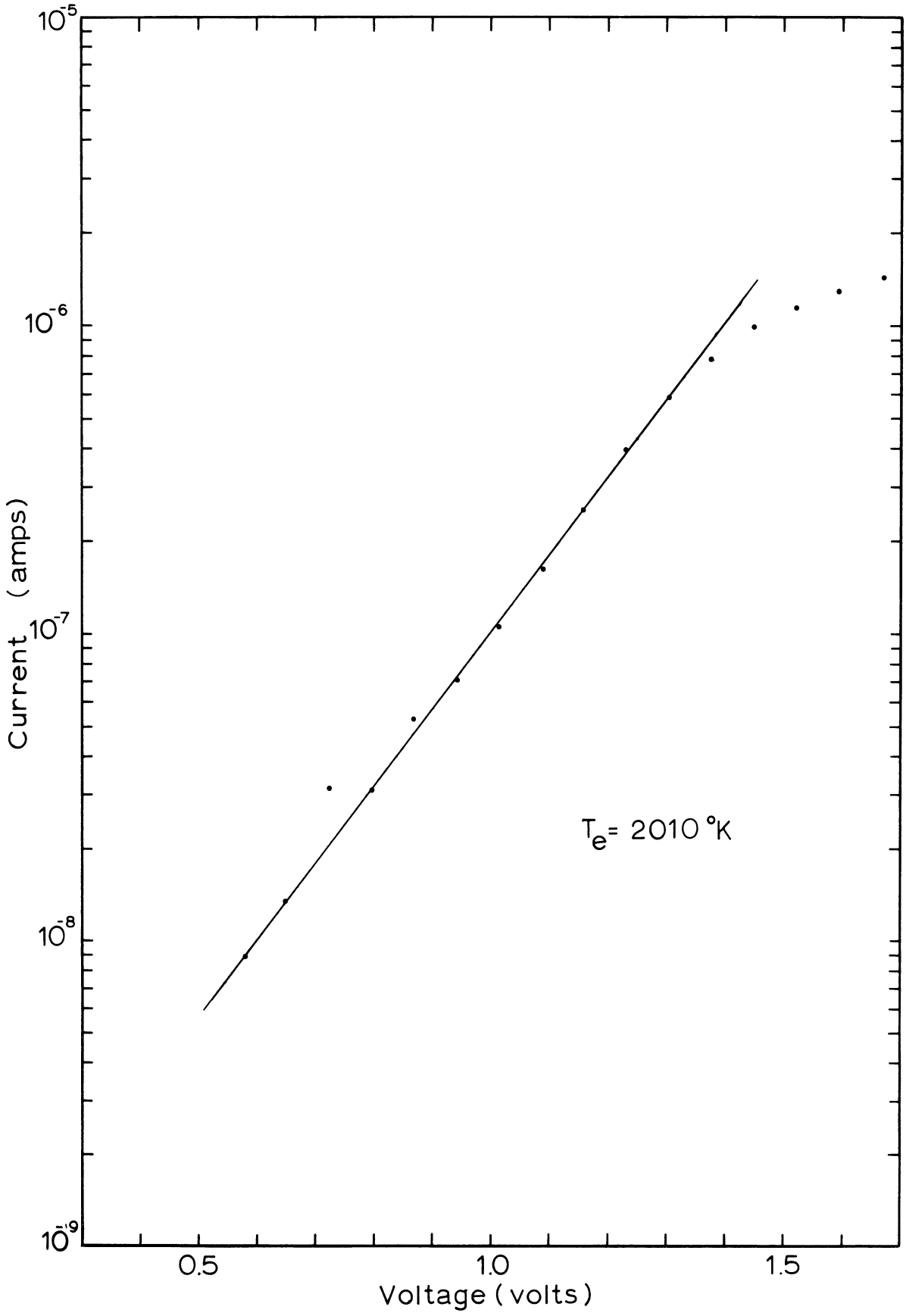

Fig. 14. T_e determination, NASA 8.19, 504 kilometers.

(Method II) for the determination of the electron density and the TP potential. The method employed is simple: by noting the collected current for two different applied voltage values (selected to ensure accelerating conditions), two equations with two unknowns are obtained, which then are solved. A computer program has been written to obtain such solutions from the actual volt-ampere characteristics. Six to eight points from each curve are typically read into the computer and substituted into Eq. (3.4.7) for the number density N_e.

$$N_e = \frac{I_a}{\left(\frac{kT_e}{2\pi m_e}\right)^{1/2} qA \left[\frac{2}{\pi^{1/2}} V_o^{1/2} + \exp(V_o)\ \mathrm{erfc}(V_o^{1/2})\right]} \tag{3.4.7}$$

This equation is obtained from simple rearrangement of Eq. (3.4.2). Since N_e is assumed constant during one sweep, a value for the TP equilibrium potential, V_R, is obtained corresponding to each pair of data points. In this program a value of V_R is first calculated for all the possible combinations of pairs and from these an average value of V_R is obtained. This average value of V_R is then used to calculate the ambient electron density from each of the data points with the aid of Eq. (3.4.7). The resulting density values are then also averaged. These averaging processes minimize the reading errors.

Another method, which is a variation of the one previously described (No. II), can also be used to obtain electron density and TP potential information. This approach is again based on solving the accelerated electron current equation for V_R and N_e. Considering two points on the "accelerated" portion of the volt-ampere curves, the ratio of currents is

$$\frac{I_{a1}}{I_{a2}} = \frac{\frac{2}{\pi^{1/2}} (V_{o1})^{1/2} + \exp(V_{o1})\ \mathrm{erfc}(V_{o1})}{\frac{2}{\pi^{1/2}} (V_{o2})^{1/2} + \exp(V_{o2})\ \mathrm{erfc}(V_{o2})} = \frac{F(V_{o1})}{F(V_{o2})} \tag{3.4.8}$$

where $V_{on} = \frac{q}{kT_e} (V_{apn} + V_D)$, $\quad n = 1,2\ldots$

If the two points under consideration correspond to the maximum applied voltage, V_{apm}, and that applied voltage which brings the cylinder to the plasma potential, $|V_R|$, respectively, one can write:

$$\frac{I_{am}}{I_{er}} = F(V_{om}). \tag{3.4.9}$$

Equation (3.4.9) provides a functional relationship between I_{er} and V_R with V_{apm} as a parameter, thus:

$$I_{er} = G(V_R) \tag{3.4.10}$$

The experimental volt-ampere curve can be expressed as

$$I_k = H(V_k) \tag{3.4.11}$$

When $V_k = -V_R$, the measured current corresponds to the random current I_{er}. Thus if Eq. (3.4.10) is plotted on the same scale as the experimental curve, the two curves will intersect at one point only. At this intersection point the applied voltage is equal in magnitude and opposite in sign to V_R and the current is the random current I_{er} from which the electron density can be computed.

The electron temperature measurement technique described here has been used successfully for a number of years for both rocket and satellite applications.[8-10] This wealth of experience provides great confidence in the results. The use of the electron current characteristics for ionospheric electron density measurements, as discussed here, is a more recent approach,[11,12] nevertheless the results so far indicate that if the experimental parameters are properly selected (e.g., current detector sensitivity, voltage sweep rate, etc.) the accuracy of the density and equilibrium potential measurements is in the order of 5-10%.

3.5 DATA PROCESSING

The theory and analysis methods described in this report have been used in analyzing data obtained from four successful TP payloads launched from Wallops Island, Virginia. All four used Sparrowbee launch vehicles which attained peak altitudes of approximately 300 km. The resulting geophysical data is presented in Ref. 12.

A section of a telemetry record, obtained during the flight of NASA 6.06, is shown in Fig. 15. To date, the data have been reduced to engineering terms from records similar to this. The voltage deflections are read with data reducers, such as the Gerber GDDRS-3B. Much of the analysis to reduce these data into atmospheric parameters has been programed for computer solutions. In the near future, a data processing system will be available for use in processing the magnetic tapes of the telemetered data. Such a system in conjunction with a computer, also to be available, will considerably decrease the time and human effort involved in obtaining the desired geophysical parameters.

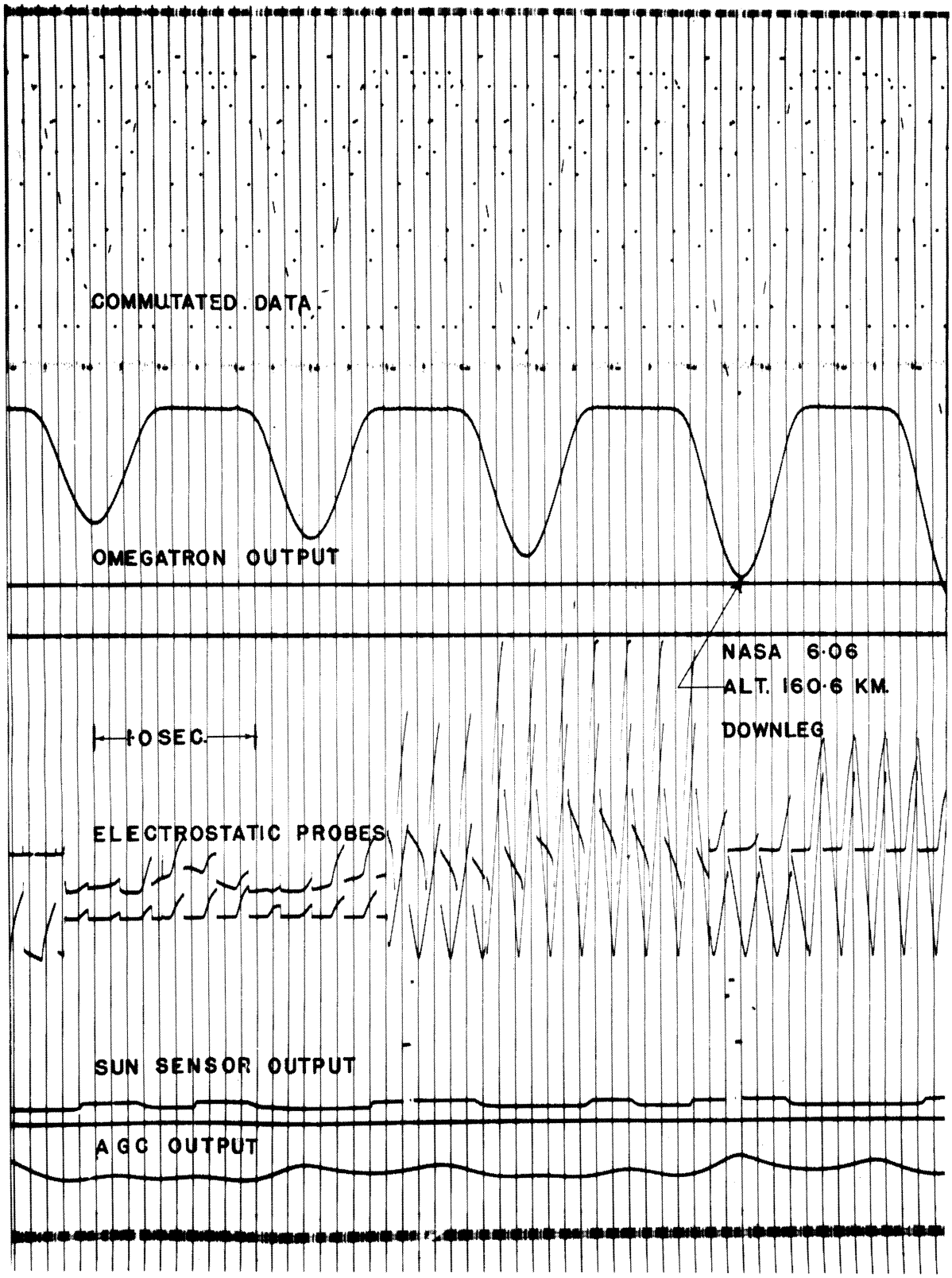

Fig. 15. Telemetry record from NASA 6.06.

REFERENCES

1. Niemann, H. B., and Kennedy, B. C. "Omegatron Mass Spectrometer for Parial Pressure Measurements in the Upper Atmosphere," (to be submitted to Rev. Sci. Inst.), 1965.

2. Carignan, G. R. and Brace, L. H., "The Dumbbell Electrostatic Ionosphere Probe: Engineering Aspects," Univ. of Mich., ORA Report 03599-6-S, Ann Arbor, November 1961.

3. Schultz, F. V., Spencer, N. W., and Reifman, A., "Atmospheric Pressure and Temperature Measurement Between the Altitude of 40 and 110 Kilometers," Upper-Air Research Program, Report No. 2, Univ. of Mich. Res. Inst. Report, Ann Arbor, July 1948.

4. Horowitz, R. and LaGow, H. E., "Upper Air Pressure and Density Measurements from 90 to 220 Kilometers With the Viking 7 Rocket," Journal of Geophysics Research, 62:57-78 (1957).

5. Nagy, A. F., Spence, N. W., Niemann, H. B., and Carignan, G. R., "Measurements of Atmospheric Pressure, Temperature, and Density at Very High Altitudes," Univ. of Mich., ORA Report 02804-7-F, August 1961.

6. Mott-Smith, H. M. and Langmuir, I. "The Theory of Collectors in Gaseous Discharges," Phys. Rev., 28, 727-763, 1926.

7. Kanal, M., "Theory of Current Collection of Moving Cylindrical Probes," J. Appl. Phys., 35, 1697-1703, 1964.

8. Spencer, N. W., Brace, L. H. and Carignan, G. R., "Electron Temperature Evidence for Nonthermal E uilibrium in the Ionosphere," J. Geophys. Res., 67, 157-175, 1962.

9. Nagy, A. F., Brace, L. H., Carignan, G. R. and Kanal M., "Direct Measurements Bearing on the Extent of Thermal Nonequilibrium in the Ionosphere," J. Geophys. Res., 68, 6401-6412, 1963.

10. Brace, L. H., Spencer, N. W., and Carignan, G. R., "Ionosphere Electron Temperature Measurements and Their Implications," J. Geophys. Res., 68, 5397-5412, 1963.

11. Nagy, A. F. and Faruqi, A. Z., "Ionospheric Electron Density and Body Potential Measurements by a Cylindrical Probe," Univ. of Mich., ORA Report 05671-4-S, September 1964.

12. Spencer, N. W., Brace, L. H., Carignan, G. R., Taeusch, D. R. and Niemann, H. B., "Electron and Molecular Nitrogen Temperature and Density in the Thermosphere," (submitted for publication, J. Geophys. Res.).